European Journal of Medicinal Chemistry 79 (2014) 164–172

Contents lists available at ScienceDirect

European Journal of Medicinal Chemistry

journal homepage: http://www.elsevier.com/locate/ejmech

Original article

Gold(I) complexes with alkylated PTA (1,3,5-triaza-7-phosphaadamantane) phosphanes as anticancer metallodrugs

Elena García-Moreno [a], Sonia Gascón [b], Elena Atrián-Blasco [a], Mª Jesus Rodriguez-Yoldi [b], Elena Cerrada [a], Mariano Laguna [a,*]

[a] Departamento de Química Inorgánica, Instituto de Síntesis Química y Catálisis Homogénea, Universidad de Zaragoza-C.S.I.C., E-50009 Zaragoza, Spain
[b] Departamento de Farmacología y Fisiología, Unidad de Fisiología, Facultad de Veterinaria, Universidad de Zaragoza, 50013 Zaragoza, CIBERobn, Spain

ARTICLE INFO

Article history:
Received 27 January 2014
Received in revised form
13 March 2014
Accepted 1 April 2014
Available online 1 April 2014

Keywords:
Gold
Thiolate
Water soluble
PTA
Antitumor properties

ABSTRACT

New stable thiolate gold(I) derivatives containing the alkylated phosphanes [PTA−CH_2Ph]Br and [PTA−CH_2COOMe]Br derived from 1,3,5-triaza-7-phosphaadamantane (PTA) have been prepared by different routes of synthesis. By the use of basic media to deprotonate the corresponding thiol in the former and by transmetallation reactions from tin (IV) complexes, in the later, thus avoiding side reactions on the phosphane. Strong antiproliferative effects are observed for most of the compounds, including the chloro- and bromo precursors with the series of phosphanes derived from PTA, in human colon cancer cell lines (Caco-2, PD7 and TC7 clones). Apoptosis-induced cell death is found for all compounds, being the thiolate derivatives with [PTA−CH_2Ph]Br the most effective, as shown by an annexin-V/propidium iodide double-staining assay.

1. Introduction

Medicinal properties of gold compounds have been exploited from ancient cultures such as India, Egypt and China [1]. Although the rational use of gold in medicine, began in the early 1920s, with the discovery of inhibitory properties of gold cyanide in Tubercle bacillus. From this moment, several diseases have been treated with gold derivatives, including tuberculosis [2] and arthritis rheumatoid [3]. Several thiolate gold(I) complexes have been used clinically in the arthritis rheumatoid treatment, namely aurothioglucose (solganol), aurothiomalate (myocrisin) [4,5] and triethylphosphine gold(I) tetraacetothioglucose (auranofin) [6,7]. In the last few decades, these derivatives and related ones have been tested against HIV for the treatment of AIDS [8,9], acute forms of asthma chronic (corticosteroid-dependent asthma), pemphigus (an autoimmune disease of the skin) [10], in treatment of malaria [11], Chagas disease [12] and cancer [13–15].

In the mid-1980s auranofin was found to show strong antiproliferation potency against cancer cells *in vitro* [16–18], as well as having limited *in vivo* antitumor activity, being only active against P388 leukemia cancer [18]. These studies have triggered an intense research on gold derivatives for cancer chemotherapy. Thus, over the last decades different type of gold-based drugs candidates have been reviewed, where different kind of ligands have been employed: phosphanes, bischelating phosphanes, thiolates, dithiocarbamates, porphyrines or N-heterocyclic carbenes [14,15,19–28].

It has been shown in gold(I) bisphosphanes, that the presence of high lipophilic character, results in severe toxicity to heart, liver and lung, as a consequence of the non-selective concentration of compounds into mitochondria of both carcinogenic and healthy cells [29–31]. Additionally, in similar gold(I) bisphosphane derivatives, a direct relationship between hepatotoxicity and lipophilicity has been found [32]. Consequently, the selectivity of such kind of derivatives for cancer over normal tissue could be improved by optimizing their lipophilic-hydrophilic balance, with the appropriate ligands [33–36]. For this reason, a balanced relationship between lipophilic and hydrophilic character is an important parameter in optimizing biodistribution, activity and selectivity of the drugs. Accordingly, water solubility of the drugs could provide such balanced relationship. The use of water-soluble phosphanes can lead to the synthesis of soluble or partially soluble complexes in water. Thus, we have previously described some water-soluble thiolate [37–40] or alkyne [41,42] gold(I) derivatives with the phosphanes PTA (1,3,5-triaza-7-phosphaadamantane), DAPTA (3,7-diacetyl-1,3,7-triaza-5-phosphabicyclo[3.3.1]nonane), sodium

* Corresponding author.
E-mail address: mlaguna@unizar.es (M. Laguna).

http://dx.doi.org/10.1016/j.ejmech.2014.04.001
0223-5234/

triphenylphosphane monosulfonate (TPPMS) or sodium triphenylphosphane trisulfonate (TPPTS), which in most of the cases have shown from moderate to excellent antiproliferative properties.

In addition, we have recently shown that the hydrophilicity of the phosphane ligand can be enhanced by alkylation of the PTA molecule, giving rise to new phosphanes with greater water solubilities compared with the free PTA and their corresponding water-soluble gold(I) compounds [43,44]. Within this frame, here we describe the synthesis of new thiolate gold(I) derivatives with some of these phosphanes derived from PTA. These complexes and their corresponding precursors, previously described by some of us [43], have been screened for their antitumor activity against human colon cancer cell lines Caco-2, as well as their apoptotic activity evaluation and their implication in the cell cycle progression.

2. Results and discussion

2.1. Synthesis and characterization

The conventional route for the synthesis of thiolate gold(I) derivatives consists of the addition of the corresponding halogen gold phosphane complex to a solution of the thiol in the presence of a base. The use of [AuBr(PTA–CH_2Ph)]Br (**1a**) leads to the isolation of the air stable solids with the formula [Au(SR)(PTA–CH_2Ph)]Br (SR = Spy, **3a**; Spyrim; **4a**, SMepyrim; **5a** and SMe_2pyrim, **6a**) (Scheme 1, *ii*) in good yields. All of them show the characteristic signals of the thiolates and those due to the [PTA–CH_2Ph]Br phosphane in their ^{1}H NMR spectra, apart from the absence of the S–*H* resonance from the starting thiol. The ^{31}P{^{1}H} NMR displays a low-field displaced singlet compared to those in the free phosphane, but at higher field with respect to the starting material [AuBr(PTA–CH_2Ph)]Br.

Treatment of [AuX(PTA–CH_2COOMe)]X (*X* = Br, **1b** or Cl, **1b′**) with the thiolates in the same conditions gave mixtures of complexes, as deducted by NMR experiments. Thus, two singlets with similar intensities are observed in their ^{31}P{^{1}H} NMR spectra and multiple signals can be detected in the ^{1}H NMR spectra. The same results are obtained independently of the basic media (KOMe/MeOH, NaOMe/MeOH, NEt_3/CH_2Cl_2 or Na_2CO_3/CH_2Cl_2). It has been recently published that PTA derivatives such as [PTA–CH_2COOMe]Br and [PTA-Me_2]$(TfO)_2$ react in the presence of the base NaOH or KOH to give the new phosphanes [PTA–CH_2COOH]Br in the former, consequently of the methyl ester transformation to carboxylic acid [44] and [PTA-Me_2] (dmoPTA) (3,7-dimethyl-1,3,7-triaza-5-phosphabicyclo[3.3.1]nonane) in the later, result of the elimination of the methylene group located between both NMe units [45,46]. In our case, the presence of a more complicated pattern than the expected in the ^{1}H NMR spectra and two resonances in the ^{31}P{^{1}H} NMR experiments could be explained by similar side reactions of the phosphane in the basic media.

Since the synthesis of thiolate complexes with the [PTA–CH_2COOMe]Br phosphane proved problematical, we decided to use an alternative route. We have focused in tin(IV) derivatives as transmetallating agents, since it has been previously shown their ability to transfer dithiolate ligands to other metals under mild conditions [47–50]. Therefore the corresponding tin thiolates, synthesized as previously described [51], were then reacted with the bromo derivative **1b** giving rise to the new thiolate gold(I) complexes [Au(SR)(PTA–CH_2COOMe)]Br (SR = Spy, **3b**; Spyrim; **4b**, SMepyrim; **5b** and SMe_2pyrim, **6b**) (Scheme 1, *iii*) as pure samples. These compounds exhibit similar ^{1}H NMR spectra than those observed in the related thiolates **3**–**6a**, with the main difference in the corresponding signals to the PTA phosphane. However a different behavior is detected in the singlets measured in the ^{31}P{^{1}H} NMR spectra, inasmuch as the resonances of the thiolates derived from [PTA–CH_2COOMe]Br are low field displaced compared with the bromo gold (I) starting material **1b** ($\delta = -41.6$ ppm), whilst upfield shifts are observed in the thiolates with [PTA–CH_2Ph]Br in comparison with [AuBr(PTA–CH_2Ph)]Br (**1a**) ($\delta = -39$ ppm).

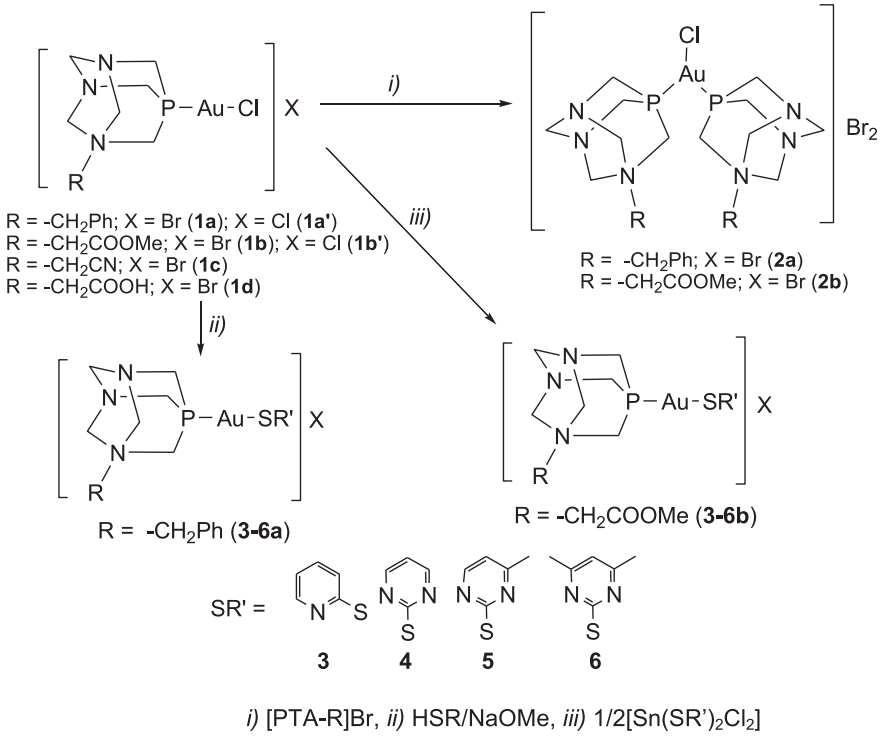

Scheme 1. Preparation of gold(I) derivatives with [PTA-R]X phosphanes.

The MALDI+ spectra for all the new thiolate gold(I) complexes with both alkylated PTA phosphanes display molecular ion peaks identified as the corresponding cation.

These new thiolate compounds resulted poorly soluble in water, with the best values ranging from 7 to 21 g L^{-1}. Curiously, although the PTA with the ester group [PTA–CH_2COOMe]Br, that is six times more water-soluble than the PTA, gave lower solubilities in the final complexes than those measured in the related with PTA [40].

2.2. Lipophilicity

As stated in the introduction, a balanced relationship between lipophilicity and hydrophilicity would be important in drug delivery process. We have measured such relationship in terms of log $D_{7.4}$ (n-octanol/water partition coefficient under physiological conditions) (Table 1) of the new thiolate derivatives and the chloro or bromo precursors depicted in Scheme 1. Complexes [AuCl(PTA–CH_2CN)]Br (**1c**) and [AuCl(PTA–CH_2COOH)]Br (**1d**) are the most hydrophilic derivatives with log $D_{7.4}$ values next to −1 (−1.04 and −0.81 respectively). However, the rest of the compounds display a balanced relationship between their lipophilic and hydrophilic character, with log $D_{7.4}$ values ranging from −0.5 and +0.18.

There is no direct relationship between the water solubility of the phosphane and the log $D_{7.4}$ value of the corresponding gold compounds since the highest hydrophilicity is not found in the complexes with the most water-soluble phosphane ([PTA–CH_2COOMe]Br). Compounds [AuCl(PTA–CH_2CN)]Br (**1c**) and [AuCl(PTA–CH_2COOH)]Br (**1d**) display the highest values of log $D_{7.4}$, −1.04 and −0.81 respectively, and the solubility in water of the PTA derivatives are up to 12 and 2.5 times lower than that found in [PTA–CH_2COOMe]Br, respectively. Accurately, these derivatives display the highest solubility in water of all complexes described herein (see Ref. [43]). Comparing the thiolate gold compounds, bearing the less soluble phosphane [PTA–CH_2Ph]Br, the liphophilicities vary with the nature of the thiolate, being more hydrophilic those with alkyl substituents in the pyrimidine ring. Similar hydrophilic character is found in all the compounds with the most water soluble phosphane [PTA–CH_2COOMe]Br, with negative values of log $D_{7.4}$ ranging from −0.26 to −0.51.

Table 1
IC_{50} values in Caco-2 cell lines and distribution coefficients of **1**–**6** complexes, auranofin and cisplatin.

Compound	Log $D_{7.4}$	IC_{50} (μM)[a]	
		Caco-2/PD7	Caco-2/TC7
[PTA–CH_2Ph]Br		91 ± 8	260 ± 12
[AuBr(PTA–CH_2Ph)]Br (**1a**)	−0.14	4.67 ± 0.02	9.86 ± 0.75
[AuCl(PTA–CH_2Ph)]Cl (**1a′**)	−0.34	4.4 ± 0.29	6.88 ± 0.6
[PTA–CH_2COOMe]Br		77 ± 5	54 ± 3
[AuBr(PTA–CH_2COOMe)]Br (**1b**)	−0.40	14.20 ± 0.81	2.11 ± 0.69
[AuCl(PTA–CH_2COOMe)]Cl (**1b′**)	−0.40	4.26 ± 0.95	11.80 ± 1.1
[PTA–CH_2CN]Br		87 ± 9	52 ± 5
[AuCl(PTA–CH_2CN)]Br (**1c**)	−1.04	4.51 ± 1.44	3.04 ± 0.85
[PTA–CH_2COOH]Br		58 ± 4	66 ± 3
[AuCl(PTA–CH_2COOH)]Br (**1d**)	−0.81	6.79 ± 1.17	0.93 ± 0.20
[AuCl(PTA–CH_2Ph)$_2$]Br_2 (**2a**)	−0.01	14.74 ± 0.22	8.48 ± 1.9
[AuCl(PTA–CH_2COOMe)$_2$]Br_2 (**2b**)	−0.01	5.53 ± 0.0045	10.17 ± 0.94
[Au(Spy)(PTA–CH_2Ph)]Br (**3a**)	0.15	4.07 ± 0.55	5.05 ± 0.05
[Au(Spyrim)(PTA–CH_2Ph)]Br (**4a**)	0.18	2.49 ± 0.02	3.95 ± 0.04
[Au(SMepyrim)(PTA–CH_2Ph)]Br (**5a**)	−0.55	6.63 ± 0.69	5.56 ± 0.02
[Au(SMe_2pyrim)(PTA–CH_2Ph)]Br (**6a**)	−0.48	1.75 ± 0.34	7.5 ± 1.5
[Au(Spy)(PTA–CH_2COOMe)]Br (**3b**)	−0.30	9.35 ± 2.1	7.67 ± 1.5
[Au(Spyrim)(PTA–CH_2COOMe)]Br (**4b**)	−0.26	4.16 ± 1.7	2.8 ± 1.0
[Au(SMepyrim) (PTA–CH_2COOMe)]Br (**5b**)	−0.51	8.11 ± 1.8	5.55 ± 1.4
[Au(SMe_2pyrim) (PTA–CH_2COOMe)]Br (**6b**)	−0.46	4.63 ± 1.3	6.37 ± 1.1
Auranofin		1.8 ± 0.1	2.1 ± 0.4
Cisplatin		37.24 ± 5.15	45.6 ± 8.08

[a] Mean ± SD of at least three determinations.

2.3. Biological studies

The precursors chloro-, bromo gold(I) derivatives (**1a**–**d**) with the phosphanes derived from PTA ([PTA-R]X, R = CH_2Ph, CH_2COOMe, CH_2CN, CH_2COOH), the chloro gold(I) bisphosphanes (**2a**–**b**), depicted in Scheme 1, and the corresponding thiolate gold complexes with the phosphanes [PTA–CH_2Ph]Br (**3**–**6a**) and [PTA–CH_2COOMe]Br (**3**–**6b**) were screened for their cytotoxic properties against human colon cancer cell lines Caco-2 (clones Caco-2/PD7, from early passage, and Caco-2/TC7, from late passage), in comparison to cisplatin and auranofin under the same experimental conditions. Cells were exposed to the metallic complexes for 72 h. The IC50 values (Table 1) were calculated by using the colorimetric mitochondrial function-based MTT viability assay (see experimental).

All the tested compounds showed comparable cytotoxicity to that observed in auranofin, but markedly lower values than those found for cisplatin. In general, exposure of Caco-2/PD7 cell lines to increasing concentrations (0–20 μM) of the complexes with the phosphane [PTA–CH_2Ph]Br led to lower IC50 values (1.75–4.67 μM) than the measured for Caco-2/TC7 cell lines (3.95–9.86 μM), except in the complexes [AuCl(PTA–CH_2Ph)$_2$]Br_2 (**2a**) and [Au(SMepyrim)(PTA–CH_2Ph)]Br (**5a**). However, the most water-soluble phosphane [PTA–CH_2COOMe]Br gives alternatively the lowest IC50 values in both cell lines and depending on the halogen, being lower for PD7 clones in the chloro compounds.

Remarkably, [Au(Spyrim)(PTA–CH_2Ph)]Br (**4a**) showed the highest cytotoxicity in both clones with low IC50 values in PD7 and TC7 cell lines (2.49 and 3.95 μM respectively), similar to auranofin and besides being 15 and 11.5 times lower than those of cisplatin. A major activity is found in all the thiolate complexes **3**–**6a/b** with the phosphanes [PTA–CH_2Ph]Br and [PTA–CH_2COOMe]Br in comparison with the halogen precursors or the bis-phosphane [AuCl(PTA–CH_2Ph)$_2$]Br_2 (**2a**) and [AuCl(PTA–CH_2COOMe)$_2$]Br_2 (**2b**).

The free phosphanes were much less effective in decreasing cancer viability over both colon cancer cell lines, with IC50 values higher than 50 μM in all the cases and even higher than 250 μM for the phosphane [PTACH_2Ph]Br in Caco-2/PD7 cell line, confirming that the gold center was necessary to obtain bioactive derivatives.

The ability of these compounds to induce apoptosis was tested by incubating both cancer cell lines Caco-2 with the gold derivatives **1**–**6**, cisplatin and auranofin for 72 h, using the annexin-V/PI double staining assay. As summarized in Table 2 and Fig. 1 compounds [AuCl(PTA–CH_2CN)]Br (**1c**), [Au(Spyrim)(PTA–CH_2Ph)]Br (**4a**) and [Au(SMepyrim)(PTA–CH_2Ph)]Br (**5a**) are the most effective with practically no live cells after 72 h of treatment in both cell lines. These derivatives are able to induce cell death by an apoptotic pathway, as derived from the higher amounts of early and late apoptosis observed in comparison to DMSO for both cancer cell lines (PD7 and TC7). In addition, the lack of significant propidium iodide uptake indicates that neither complex induces necrotic cell death after 72 h. One important difference is found in complex **4a**, that exhibits the highest amount of late-stage apoptosis compared to **1c** and **5a** (61.2% versus 36.8 and 22.6%, respectively) in Caco-2/PD7 cells and similar amounts in early and late-stage apoptosis in Caco-2/TC7 clone (approx. 47%). The remaining thiolate derivatives [Au(Spy)(PTA–CH_2Ph)]Br (**3a**) and [Au(SMe_2pyrim)(PTA–CH_2Ph)]Br (**6a**) differ from **4a** and **5a** mainly in the population of live cells in both clones, giving higher amounts (40.3%

Table 2
Summary of the effects of treating PD7 and PC7 cell lines with the metallic compounds **1**–**6**, cisplatin and auranofin after 72 h. [AuBr(PTA–CH_2Ph)]Br (**1a**), [AuCl(PTA–CH_2Ph)]Cl (**1a′**), [AuBr(PTA–CH_2COOMe)]Br (**1b**), [AuCl(PTA–CH_2COOMe)]Cl (**1b′**), [AuCl(PTA–CH_2CN)]Br (**1c**), [AuCl(PTA–CH_2COOH)]Br (**1d**), [AuCl(PTA–$CH_2Ph)_2$]Br_2 (**2a**), [AuCl(PTA–$CH_2COOMe)_2$]Br_2 (**2b**), [Au(Spy)(PTA–CH_2Ph)]Br (**3a**), [Au(Spyrim)(PTA–CH_2Ph)]Br (**4a**), [Au(SMepyrim)(PTA–CH_2Ph)]Br (**5a**), [Au(SMe_2pyrim)(PTA–CH_2Ph)]Br (**6a**), [Au(Spy)(PTA–CH_2COOMe)]Br (**3b**), [Au(Spyrim)(PTA–CH_2COOMe)]Br (**4b**), [Au(SMepyrim)(PTA–CH_2COOMe)]Br (**5b**), [Au(SMe_2pyrim)(PTA–CH_2COOMe)]Br (**6b**).

Complex	PD7				TC7			
	Live (%)	Early apoptosis	Late apoptosis	Necrosis (%)	Live (%)	Early apoptosis	Late apoptosis	Necrosis (%)
1a	52.4	17.3	21.4	8.9	72.2	6.7	17.0	4.1
1a′	53.3	14.1	18.4	14.2	69.3	26.0	8.7	19.4
1b	59.8	6.6	17.5	16.2	76.7	3.0	9.9	10.5
1b′	58.1	14.0	19.8	8.1	77.9	2.8	13.2	6.1
1c	5.0	55.0	36.8	3.2	4.4	79.6	15.7	0.3
1d	75.4	8.6	9.7	6.3	87.7	4.9	4.0	3.3
2a	14.3	4.41	43.7	0.6	12.0	47.5	39.6	0.9
2b	31.3	31.5	36.7	0.5	59.8	20.7	18.7	0.8
3a	40.3	15.2	37.0	7.5	45.9	13.3	36.8	4.0
4a	0.5	37.4	61.2	0.9	1.5	47.2	47.9	3.4
5a	0.3	77.0	22.6	0.0	0.5	34.1	35.3	0.1
6a	34.7	45.8	19.2	0.4	49.7	43.1	6.8	0.4
3b	80.2	6.8	8.9	4.1	77.9	7.2	7.7	7.2
4b	81.1	5.7	7.8	5.5	82.2	3.8	6.2	7.2
5b	66.7	10.4	16.5	6.4	80.9	9.6	7.8	1.7
6b	80.1	4.9	9.8	5.2	83.0	7.2	6.8	3.1
Cisplatin	55.4	7.6	22.4	14.6	82.0	3.3	8.8	6.0
Auranofin	37.4	7.7	32.2	22.7	0.0	18.3	81.5	0.2
DMSO	89.9	3.2	5.8	1.1	88.1	2.7	5.7	3.5

and 34.7% in PD7; 45.9% and 49.7% in TC7, respectively) to those measured in **4a** and **5a**. Induction to apoptosis is also observed in these thiolate compounds as well as in the bis-phosphane derivatives [AuCl(PTA–$CH_2Ph)_2$]Br_2 (**2a**) and [AuCl(PTA–$CH_2COOMe)_2$]Br_2 (**2b**), along with no significant necrotic population. Less effectiveness can be deduced in the chloro or bromo-gold derivatives **1a**, **1a′**, **1b**, **1b′**, **1d** and the thiolate **3**–**6b** with [(PTA–CH_2COOMe)]Br that behave similarly to cisplatin where high amount of live population remains after 72 h of treatment in addition to a moderate percentage of apoptotic cells.

To evaluate a possible influence of the gold derivatives on the cell cycle, we analyzed the cell cycle progression and DNA fragmentation in surviving cells, following drug exposure by PI staining and flow cytometric analyses in both cancer cell lines after 72 h of treatment with complexes **1**–**6**, cisplatin and auranofin. Complexes [AuCl(PTA–CH_2CN)]Br (**1c**), [AuCl(PTA–$CH_2Ph)_2$]Br_2 (**2a**), [Au(Spyrim)(PTA–CH_2Ph)]Br (**4a**), [Au(SMepyrim)(PTA–CH_2Ph)]Br (**5a**) and auranofin led to a markedly perturbed flow cytometry profile, most likely due to extensive cell death. Accurately these derivatives give the lowest percentages for live cells after 72 h of complex treatment (see Table 2 and Fig. 1). Fig. 2 shows a histogram of Caco-2/PD7 and Caco-2/TC7 cells treated with DMSO and the complexes in which it was possible to determine the percentages of G_1-, S- and G_2-phase cells.

Treatment of Caco-2/PD7 cells with complexes **1a**, **1a′**, **1b**, **1b′**, **3a**, **6a**, **3**–**6b** and cisplatin did not significantly affect the cell cycle after 72 h incubation, where the majority of the cells are in the G_1 and S-phases. Only [AuCl(PTA–$CH_2COOMe)_2$]Br_2 (**2b**) displayed a variation worthy of mention in the treatment with Caco-2/PD7 cells with an appreciable increase in the population of S-phase with a decrease in the G_1- and G_2-phases. A slight increase in the population in the G_1-phase, resulting in a concomitant decrease in the S-phase is detected in complexes **1a**, **1a′** and **1b** after incubation with TC7 clone, that could prevent the entry of cells into the subsequent S and G_2/M phases. This fact could be in accordance with the highest values of necrotic population measured in these derivatives (8.9–16.2%, Table 2).

To evaluate the reactivity of the gold derivatives with DNA, we monitored their influence on pIRES2-EGFP (5308 pb) plasmid DNA, following incubation at 37 °C, by agarose gel electrophoresis, in the particular case of the most active complex: [Au(Spyrim)(PTA–CH_2Ph)]Br (**4a**) and compared to cisplatin (see Supporting Information). Treatment with increasing amounts of the gold complex does not affect the mobility of the plasmid, conversely with the observed in cisplatin. The lack of reactivity with DNA is comparable to that observed for auranofin and in previously reported gold(I) derivatives [41,52].

Finally, the stability of [Au(Spyrim)(PTA–CH_2Ph)]Br (**4a**) against both cancer cell lines under physiological conditions was analyzed by absorption spectroscopy (Fig. 3). A solution suitable for spectrophotometric analysis was prepared by diluting a DMSO mother solution of the complex with aqueous buffer PBS. Complex **4a** is characterized by an intense band at 290 nm, which remains unchanged over 24 h of the study under incubation of the solution at 37 °C. Neither band shifts nor additional bands at around 550 nm, characteristic of metallic gold formation, are detected during the experiment, which clearly showed that this complex is essentially stable for at least 24 h in PBS solution at 37 °C. In addition a control NMR experiment was performed under buffer conditions (PBS/d_6-DMSO/D_2O solution) (see supporting information for more details). The addition of the buffer solution in water gives the released of the phosphane [(PTA–CH_2Ph)]Br, which is immediately oxidized, as evidenced by the $^{31}P\{^1H\}$ NMR with the appearance of the corresponding signal of the oxide. The signals observed in the ^1H NMR remain intact after 24 h in PBS solution. The dissociation of the phosphane (PEt_3) and subsequent oxidation is also observed in auranofin when is added to blood, as a consequence of its reaction with cysteine-34 residue present in the serum albumin [14]. The predisposition of complex **4a** to dissociate the phosphane under physiological conditions could facilitate the following reactions with biomolecules thus justifying its high antitumor activity.

In general, the mechanism of biological action of gold derivatives is still not fully elucidated. Although new protein targets for these compounds are emerging, for instance zinc-finger proteins, aquaporins, carbonic anhydrases among others [53–55], the activity of gold compounds is often associated with the inhibition of the seleno-enzyme thioredoxin reductase (TrxR) [20,56–59]. This inhibition can disturb mitochondrial function and generate elevated ROS levels, leading to a decrease in the mitochondrial membrane potential [60]. We have previously shown the inhibition

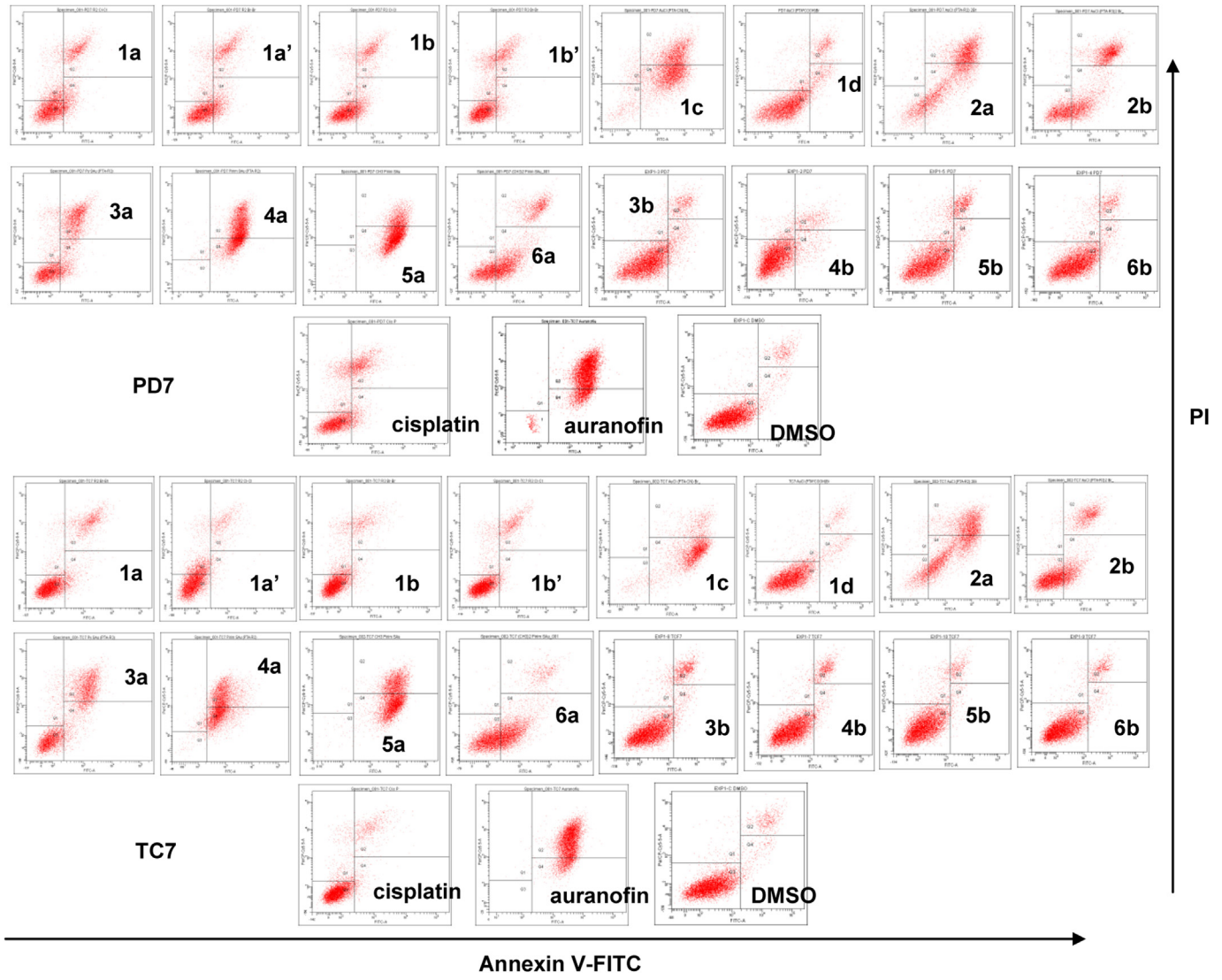

Fig. 1. Quantitative flow cytometry analyses using propidium iodide (PI) uptake and annexin-V staining in PD7 and TC7 colon cancer cells treated with DMSO, 20 μM in complexes **1**–**6**, cisplatin and auranofin after 72 h.

of cytosolic and mitochondrial thioredoxin reductases by related thiolate derivatives with PTA [39]. Although additional studies will be conducted on the new thiolate compounds, we can imagine a similar behavior to the found in the reported derivatives.

3. Conclusions

Two different routes of synthesis of thiolate gold(I) with water soluble phosphanes derived from PTA [PTA–CH_2Ph]Br and [PTA–CH_2COOMe]Br are included in the paper. The conventional way by deprotonating the thiol in basic media led to mixtures in the case of [PTA–CH_2COOMe]Br due to side reactions, which is avoided by using transmetallating reactions starting from tin(IV) thiolates. These new thiolates, their corresponding chloro- and bromo-precursors and chloro gold(I) derivatives with similar phosphanes have been tested for their antiproliferative activity against the human colon cancer cell line Caco-2 (PD7 and TC7 clones). All the compounds showed comparable cytotoxicity to auranofin and remarkably better than cisplatin. Although all the thiolate gold(I) derivatives appeared to be the most effective complexes, only those bearing the phosphane [PTA–CH_2Ph]Br induced apoptosis more efficiently, giving to low amounts of live population and high percentages of apoptotic cells after 72 h of treatment. A balanced relationship between hidrophilicity and lipophilicity is found in all the complexes with the phosphanes [PTA–CH_2Ph]Br and [PTA–CH_2COOMe]Br, however the use of [PTA–CH_2CN]Br or [PTA–CH_2COOH]Br led to more hydrophilic character, with log $D_{7.4}$ next to −1. Complex [Au(Spyrim)(PTA–CH_2Ph)]Br (**4a**), which resulted the most effective in both cell lines, is essentially stable under PBS buffer solution at 37 °C as deduced from absorption spectroscopy. Since this complex did not damage DNA and displayed predisposition to dissociate the phosphane under PBS buffer solution, its *in vitro* effectiveness might be due to interactions with critical proteins/enzymes in keeping with other gold complexes.

4. Experimental section

4.1. General procedures

^{1}H, ^{31}P{^{1}H} (161.97 MHz) and ^{13}C{^{1}H} (100.62 or 75.4 MHz) NMR spectra were recorded on 400 MHz or 300 MHz Bruker Avance

spectrometers. Chemical shifts are quoted in ppm relative to external TMS (^{1}H, ^{13}C) or 85% H_3PO_4 (^{31}P); coupling constants are reported in hertz. MALDI mass spectra were measured on a Micromass Autospec spectrometer in positive ion mode using *trans*-2-[3-(4-*tert*butylphenyl)-2-methyl-2-propenylidene]malonitrile (DCTB) as the matrix. IR spectra were recorded on a Perkin–Elmer Spectrum 100 FTIR (far-IR) spectrophotometer. Elemental analyses were obtained in-house using a LECO CHNS-932 microanalyzer. The gold derivatives [AuCl(PTA-R)]X (R = $-CH_2Ph$ (**1a,a′**), $-CH_2COOMe$ (**1b,b′**), $-CH_2CN$ (**1c**), $-CH_2COOH$ (**1d**); *X* = Br or Cl) were prepared as published elsewhere [44]. The thiolato tin(IV) [$SnMe_2$(SR)] (R = compounds) were prepared as similar previously described complexes [51,61].

4.2. Synthesis

4.2.1. General synthesis of [Au(SR)(PTA–CH_2Ph)]Br (SR = Spy, **3a**; Spyrim, **4a**; SMepyrim, **5a**; SMe_2pyrim, **6a**)

To a solution of KOH (0.55 mmol) in MeOH (ca. 10 mL) containing the thiol compound (0.5 mmol) was added [AuBr(PTA–CH_2Ph)]Br (0.5 mmol). After stirring the mixture for ca. 12 h at room temperature the solutions were evaporated under vacuum to dryness and the residue extracted in dichloromethane (3 × 10 mL). The combined extracts were passed through Celite and concentrated under vacuum to *ca.* 5 mL. Addition of Et_2O allowed the precipitation of the products, which were isolated by filtration and dried in air.

The following complexes were prepared using this method.

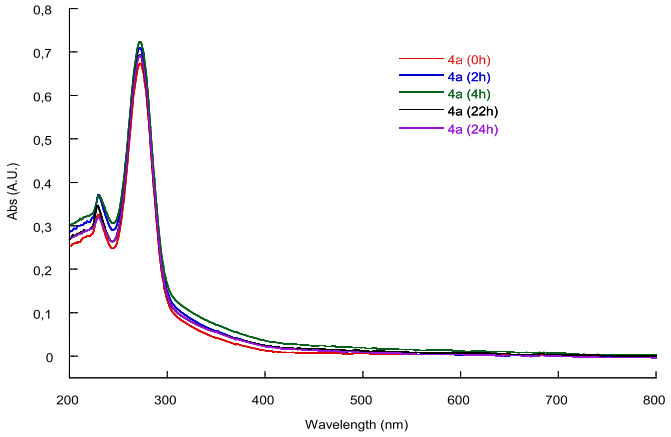

Fig. 3. Hydrolysis profile of complex [Au(Spyrim)(PTA–CH_2Ph)]Br (**4a**) under phosphate buffer 10 mM pH 7.4. Spectra were recorded at different times over 24 h at 37 °C.

*4.2.1.1. [Au(Spy)(PTA–CH_2Ph)]Br (**3a**).* Pale yellow solid in 68% yield. ^{1}H RMN (400 MHz, dmso-d_6, 25 °C): δ = 8.09 (d, 1H, J_{HH} = 4 Hz, *py*), 7.59–7.54 (m, 5H, *Ph*), 7.37–7.35 (m, 2H, *py*), 6.87 (t, J_{HH} = 5.6 Hz, 1H, *py*), 5.18 and 4.97 (AB system, 4H, J_{AB} = 11.6 Hz, NCH_2N), 4.7–4.56 (m, 3H, PCH_2N + NCH_2N), 4.43–4.24 (m, 2H, PCH_2N), 4.26 (s, 2H, CH_2Ph), 4.16–4.07 (m, 3H, PCH_2N + NCH_2N). $^{31}P\{^{1}H\}$ RMN (dmso-d_6): δ: −40.1 ppm. MALDI MS: *m/z* 556 $[M]^+$ (18%). I.R.: ν(S–Au): 551 cm^{-1}. $C_{18}H_{23}AuBrN_4O_2PS$ (634.04): C

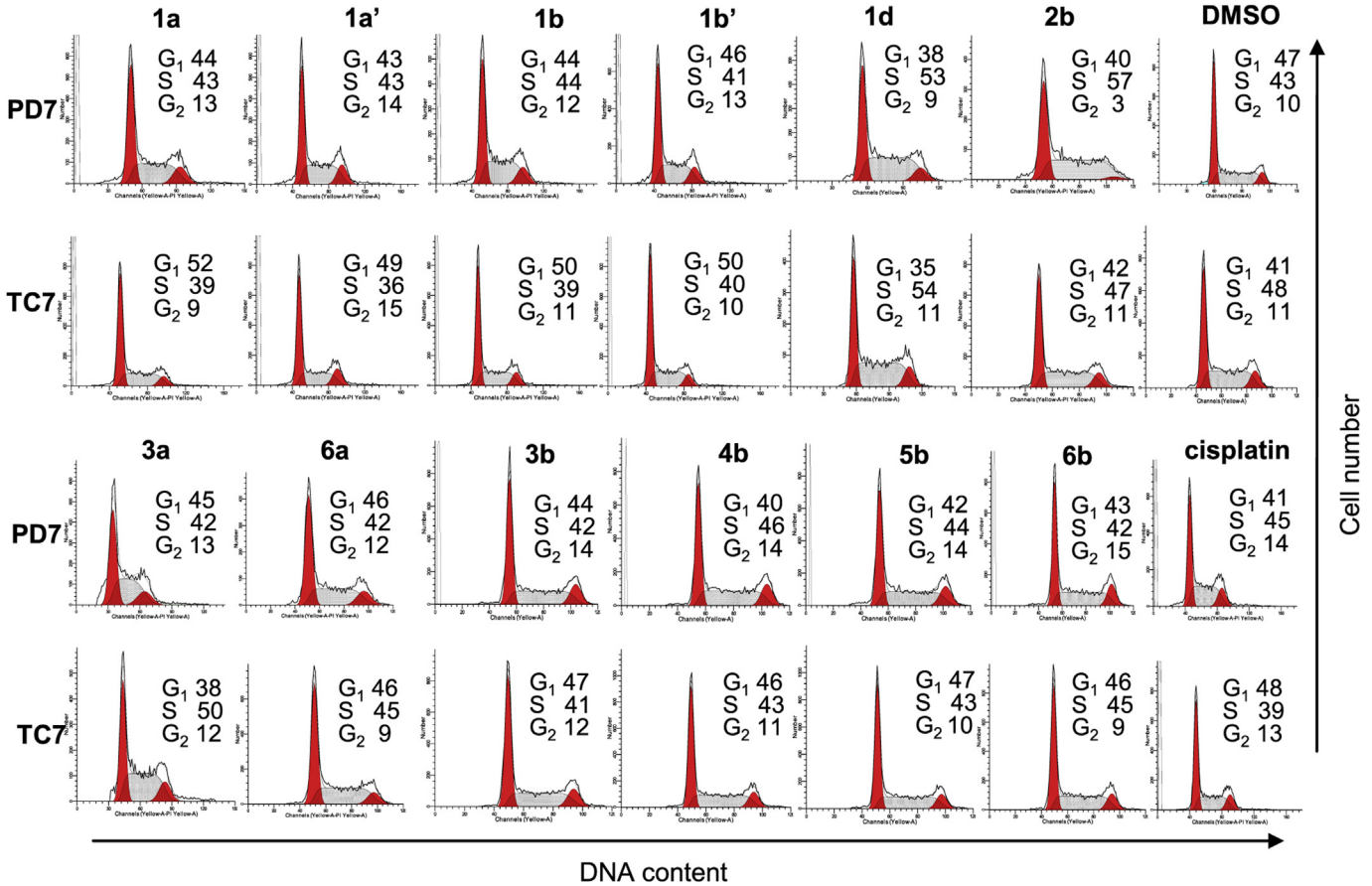

Fig. 2. Cell-cycle analysis after treatment with the metal complexes for 72 h. Cell cycle and DNA fragmentation were determined by propidium iodide staining, showing the corresponding percentages of G_1-, S- and G_2-phase cells.

34.03, H 3.65, N 8.82; found: C 33.76, H 3.38, N 9.12. S_{25° (H_2O): 6.76 g L^{-1}.

*4.2.1.2. [Au(Spyrim)(PTA–CH_2Ph)]Br (**4a**).* Yellow solid in 86% yield. ^{1}H NMR (400 MHz, MeOD, 25 °C): δ = 8.34 (d, 2H, J_{HH} = 4.8 Hz, *pyrim*), 7.59–7.54 (m, 5H, Ph), 7.02 (t, 1H, J_{HH} = 4.9 Hz, *pyrim*), 5.14 and 4.94 (AB system, 4H, J_{AB} = 12 Hz, NCH_2N), 4.67 (d, 2H; J_{HH} = 13.7 Hz, NCH_2N), 4.48 (d, J_{HH} = 13.2 Hz, 2H, PCH_2N), 4.38 (s, 2H, CH_2Ph), 4.18–4.08 (m, 2H, PCH_2N), 4.00–3.95 (m, 2H, PCH_2N). ^{31}P{^{1}H} NMR MeOD: δ (ppm) = −66.13 (s) ppm. ^{13}C{^{1}H} NMR (75 MHz, dmso-d_6): δ = 133.48, 130.70, 130.34, 129.5 (*Ph*); 156.82 (*Spyrim*); 79.8 (s, NCH_2N); 69.4 (s, NCH_2N); 55.7 (d, J_{PC} = 25.87 Hz, PCH_2N); 46.0 (d, J_{PC} = 15.67 Hz, PCH_2N, 2C); 49.3 (s, CH_2Ph). MALDI MS (*m*/*z*): 556 [M]$^+$ (20%). IR ν(S–Au): 567 cm^{-1}. $C_{17}H_{22}AuBrN_5PS$ (636.3): C 32.09, H 3.48, N 11.01; found: C 32.16, H 3.31, N 11.40. S_{25°, H_2O < 0.1 g L^{-1}.

*4.2.1.3. [Au(SMepyrim)(PTA–CH_2Ph)]Br (**5a**).* Yellow solid in 75% yield. ^{1}H NMR (400 MHz, dmso-d_6, 25 °C): δ = 8.12 (d, 1H, J_{HH} = 6.8 Hz, *pyrim*), 7.38–7.22 (m, 5H, Ph), 6.73 (d, 1H, J_{HH} = 6.8 Hz, *pyrim*), 4.92 and 4.82 (AB system, J_{AB} = 16 Hz, 4H, NCH_2N), 4.52 and 4.31 (AB system, 2H, J_{AB} = 16.4 Hz, NCH_2N), 4.39–4.36 (m, 1H, NCH_2P), 4.21 (s, 2H, CH_2Ph), 3.99–3.90 (m, 2H, NCH_2P), 3.79–3.65 (m, 3H, NCH_2P). ^{31}P{^{1}H} NMR MeOD: δ = −47.8 (s) ppm. ^{13}C{^{1}H} NMR (100.72 MHz, dmso-d_6): δ (ppm) = 166.15 (s, *SMepyrim*), 129.39, 128.95, 128.48, 127.74 (*Ph*), 114.46 (s, *SMepyrim*), 80.1 (s, NCH_2N), 70.56 (s, NCH_2N), 55.45 (d, J_{PC} = 26 Hz, PCH_2N), 46.0 (s, Me), 45.6 (d, J_{PC} = 26.4 Hz, PCH_2N, 2C). MALDI MS (*m*/*z*): 570 [M]$^+$ (40%). IR ν(S–Au): 571 cm^{-1} $C_{18}H_{24}AuBrN_5PS$ (650.3): C 33.24, H 3.72, N 10.77; found: C 33.16, H 3.45, N 10.72. S_{25°, H_2O < 0.1 g L^{-1}.

*4.2.1.4. [Au(SMe$_2$pyrim)(PTA–CH_2Ph)]Br (**6a**).* Yellow solid in 75% yield, ^{1}H NMR (400 MHz, dmso-d_6, 25 °C): δ = 7.62–7.55 (m, 5H, *Ph*), 6.96 (s, 1H, *pyrim*), 5.29 and 4.04 (AB system, 4H, J_{AB} = 12 Hz, NCH_2N), 5.24–5.22 (m, 2H, NCH_2N), 4.90 (d, 2H, J = 11.6 Hz, PCH_2N), 4.8–4.79 (m, 2H, PCH_2N), 4.67–4.64 (m, 2H, PCH_2N), 4.26 (s, 2H, CH_2Ph), 2.72 (s, 6H, 2Me). ^{31}P{^{1}H} NMR (dmso-d_6): δ = −42.7 (s) ppm. ^{3}C{^{1}H} NMR (100.72 MHz, dmso-d_6): δ (ppm) = 128.9, 128.14, 121.24 (*Ph*), 115.57 (s, *SMe$_2$pyrim*), 79.9 (s, NCH_2N), 56.3 (d, J_{PC} = 25 Hz, PCH_2N), 49.5 (s, *Me*), 47.5 (d, J_{PC} = 26 Hz, PCH_2N). MALDI MS (*m*/*z*): 559 [M]$^+$ (40%). IR ν(S–Au): 567 cm^{-1}. $C_{19}H_{26}AuBrN_5PS$ (664.35): C 34.35, H 3.94, N 10.54; found: C 33.96, H 3.79, N 10.75. S_{25°, H_2O < 0.1 g L^{-1}.

*4.2.2. General synthesis of [Au(SR)(PTA–CH_2COOMe)]Br (SR = Spy, **3b**; Spyrim, **4b**; SMepyrim, **5b**; SMe$_2$pyrim, **6b**)*

To a solution of [AuBr(PTA–CH_2CO_2Me)]Br (0.5 mmol) in MeOH (ca. 10 mL) under argon atmosphere [Sn(SR)$_2$Me$_2$] (0.25 mmol) was added. After stirring the mixture for ca. 4 h at room temperature the solutions were concentrated under *vacuum*. Addition of Et_2O allowed the precipitation of the products, which were isolated by filtration and dried in air.

Using this method the following complexes were prepared:

*4.2.2.1. [Au(Spy)(PTA–CH_2COOMe)]Br (**3b**).* Pale yellow solid in 65% yield. ^{1}H RMN (400 MHz, dmso-d_6, 25 °C): δ = 7.93 (s, br, 1H, *Spy*), 7.42 (t, 1H, J_{H-H} = 8 Hz, *Spy*), 7.35 (d, 1H, J_{H-H} = 8.6 Hz, *Spy*), 6.85 (t, J_{H-H} = 6 Hz, 1H, *Spy*), 5.40 and 5.26 (AB system, 4H, J_{AB} = 11.2 Hz, NCH_2N), 5.01 (s, 2H, NCH_2P), 4.62–4.58 (m, 1H, NCH_2N), 4.41–4.20 (m, 5H, NCH_2P + NCH_2N), 4.17 (s, 2H, CH_2COOMe), 3.79 (s, 3H, COO*Me*). ^{31}P{^{1}H} RMN (dmso-d_6): δ = −38.8 (s,br) ppm. ^{13}C{^{1}H} NMR (75.4 MHz, dmso-d_6): δ = 164.55 (s, *C*=O), 129.7, 132.90, 137.37 (s, *Spy*), 80.4 (s, NCH_2N), 59.59 (s, CH_2COOMe), 54.35 (s, NCH_2P), 53.56 (s, *Me*), 48.09 (d, J_{PC} = 14 Hz, NCH_2P). MALDI MS: *m*/*z* 537[M]$^+$ (100). I.R.: ν(C=O): 1744 cm^{-1}. $C_{14}H_{21}AuBrN_4O_2PS$ (617.25): C 27.24, H 3.43, N 9.08; found: C 27.16, H 3.41, N 9.42. S_{25°, H_2O < 0.1 g L^{-1}.

*4.2.2.2. [Au(Spyrim)(PTA–CH_2COOMe)]Br (**4b**).* Pale yellow solid in 83% yield. ^{1}H RMN (400 MHz, dmso-d_6, 25 °C): δ = 8.35 (d, 2H, J_{H-H} = 4.6 Hz, *pyrim*), 6.98 (t, 1H, *pyrim*), 5.45 and 5.30 (AB system, 4H, J_{AB} = 11.2 Hz, NCH_2N), 5.06 (s, 2H, NCH_2N); 4.66–4.63 (m, 1H, NCH_2P), 4.46–4.34 (m, 5H, NCH_2P), 4.21 (s, 2H, CH_2COOMe), 3.79 (s, 3H, COO*Me*). ^{31}P{^{1}H} RMN (dmso-d_6): δ: −36.8(s) ppm. ^{13}C{^{1}H} NMR (75.4 MHz, dmso-d_6): δ = 164.55 (s, *C*=O), 157.6, 116.39 (s, *pyrim*), 80.52 (s, NCH_2N), 69.03 (d, J_{PC} = 5 Hz, NCH_2P), 59.64 (s, CH_2COOMe), 54.41 (s, NCH_2N), 53.6 (s, *Me*), 48.13 (d, J_{PC} = 15 Hz, NCH_2P). I.R.: ν(C=O): 1745 cm^{-1}. MALDI MS (*m*/*z*): 539 [M]$^+$ (15). $C_{13}H_{20}AuBrN_5O_2PS$ (618.24): C 25.26, H 3.26, N 11.33; found: C 25.05, H 3.21, N 11.27. S_{25°, H_2O: 21 g L^{-1}.

*4.2.2.3. [Au(SMepyrim)(PTA–CH_2COOMe)]Br (**5b**).* Pale yellow solid in 80% yield. ^{1}H RMN (400 MHz, dmso-d_6, 25 °C): δ = 8.18 (d, 1H, J_{H-H} = 4 Hz, *pyrim*), 6.86 (d, 1H, J_{H-H} = 3.9 Hz *pyrim*), 5.44 and 5.33 (AB system, 4H, J_{AB} = 11.2 Hz, NCH_2N), 5.17–5.05 (m, 2H, NCH_2P), 4.57–4.42 (m, 6H, NCH_2N + NCH_2P), 4.22 (s, 2H, CH_2COOMe), 3.78 (s, 3H, COOMe), 2.28 (s, 3H, *SMe*pyrim). ^{31}P{^{1}H} RMN (dmso-d_6): δ = −31.3(s) ppm. ^{13}C{^{1}H} NMR (75.4 MHz, dmso-d_6): δ = 164.5(s, *C*=O), 125.8, 117 (s, *pyrim*), 80.5 (s, NCH_2N), 69.0 (s, NCH_2N), 59.5 (s, CH_2COOMe), 54.2 (d, J_{PC} = 18 Hz NCH_2P), 53.5 (s, Me), 47.8 (d, J_{PC} = 20 Hz, NCH_2P), 26.3 (s, *Me*pyrim). MALDI MS (*m*/*z*): 553 [M]$^+$ (18). I.R.: ν(C=O): 1745 cm^{-1}. $C_{14}H_{22}AuBrN_5O_2PS$ (632.27): C 26.59, H 3.51, N 11.08; found: C 26.26, H 3.31, N 11.07. S_{25°, H_2O: 15 g L^{-1}.

*4.2.2.4. [Au(SMe$_2$pyrim)(PTA–CH_2COOMe)]Br (**6b**).* Pale yellow solid in 74% yield. ^{1}H RMN (400 MHz, dmso-d_6, 25 °C): δ = 6.75 (s, 1H, *pyrim*), 5.40 and 5.26 (AB system, 4H, J_{AB} = 11.2 Hz, NCH_2N), 5.02 (s, 2H, NCH_2P), 4.63–4.60 (m, 1H, NCH_2N), 4.44–4.37 (m, 5H, NCH_2N + NCH_2P), 4.17 (s, 2H, CH_2COOMe), 3.79 (s, 3H, COO*Me*), 2.22 (s, 6H, *Me*pyrim).^{31}P{^{1}H} RMN (dmso-d_6): δ: −36.5 (s, br) ppm. ^{13}C{^{1}H} NMR (75.4 MHz, dmso-d_6): δ = 164.5 (s, *C*=O), 118.6 (s, *pyrim*), 80.39 (s, NCH_2N), 69.0 (s, NCH_2N), 59.57 (s, CH_2COOMe), 54.3 (d, J_{PC} = 11 Hz, NCH_2P), 53.9 (s, Me), 48.2 (d, J_{PC} = 16.5 Hz, NCH_2P), 24.4 (s, *Me*pyrim). MALDI MS (*m*/*z*): 567 [M]$^+$ (17). IR ν(C=O): 1745 cm^{-1}. $C_{15}H_{24}AuBrN_5O_2PS$ (646.29): C 27.88, H 3.74, N 10.84; found: C 27.66, H 3.71, N 10.72. S_{25°, H_2O: 10 g L^{-1}.

4.3. Distribution coefficients (log $D_{7.4}$)

The n-octanol-water partition coefficients of the complexes were determined as previously reported [62] using a shake-flask method. PBS buffered distilled water (100 mL, phosphate buffer [PO_4^{3-}] = 10 μM, [NaCl] = 0.15 M, pH 7.4) and n-octanol (100 mL) were saturated for 72 h. 1 mg of the complexes was mixed in 1 mL of aqueous and organic phase, respectively for 10 min. The resultant emulsion was centrifuged to separate the phases. The concentration of the compound in each phase was determined using UV absorbance spectroscopy. Log $D_{7.4}$ was defined as log{[compound$_{(organic)}$]/[compound$_{(aqueous)}$]}.

4.4. In vitro assays

4.4.1. Cell viability assay

Human Caco-2 cell line PD7 and TC7 clones were kindly provided by Dr. Edith Brot-Laroche (Université Pierre et Marie Curie-Paris 6, UMR S 872, Les Cordeliers (France)). Caco-2 cells were maintained in a humidified atmosphere of 5% CO_2 at 37 °C. Cells (passages 50–80) were grown in Dulbecco's Modified Eagles medium (DMEM) (Gibco Invitrogen, Paisley, UK) supplemented with 20% fetal bovine serum (FBS), 1% non essential amino acids, 1%

penicillin (1000 U/ml), 1% streptomycin (1000 μg/mL) and 1% amphotericin (250 U/ml). Experiments were performed 24 h post-seeding.

Stock solutions of the complexes (saline solution or DMSO) were diluted in complete medium to the required concentration. DMSO at similar concentrations did not show any effects on cytotoxicity.

For cytotoxicity screening experiments, cells were seeded in 96-well plates at a density of 4×10^3 cells/well. The culture medium was replaced with fresh medium (without FBS) containing the complexes at concentrations varying from 0 to 20 μM, with an exposure time of 72 h. Thereafter, the cell survivals were measured using the MTT test as previously described [63]. The assay is dependent on the cellular reduction of 3-(4,5-dimethyl-2-thiazoyl)-2,5-diphenyltetrazolium bromide (MTT, Merck) by the mitochondrial dehydrogenase of viable cells to a blue formazan product which can be measured spectrophotometrically. Following appropriate incubation of cells, with or without the metallic complexes, MTT was added to each well in an amount equal to 10% of the culture volume and gentle stirring in a gyratory shaker which enhances dissolution and incubation was continued 37 °C for 4 h. Thereafter the medium and MTT are removed and DMSO is added to each well. At the end, the results are obtained by measuring absorbance with a scanning multiwell spectrophotometer (BIOTEX SINERGY HT SIAFRTD) at wavelength of 560/670 nm and compared to the values of control cells incubated in the absence of complexes. Experiments were conducted in quadruplicate wells and repeated at least three times.

4.4.2. Measurements of apoptosis

Human Caco-2 cell line PD7 and TC7 clones were exposed for 72 h with 20 μM of the metallic compounds, collected and stained with Annexin V-FTIC according to manufacturer's recommendation. A negative control was prepared by unreacted cells, that was used to define the basal level of apoptotic and necrotic or dead cells. After incubation, cells were transferred to flow-cytometry tubes and washed twice with temperate phosphate-buffered saline (PBS) and resuspended in 100 μL Annexin V binding buffer (10 mM Hepes/NaOH, pH 7.4, 140 mM NaCl, 2.5 mM $CaCl_2$), 5 μL of the Annexin V-FITC and 5 μL of PI to each 100 μL of cell suspension. After incubation for 15 min at room temperature in the dark, 400 μL of 1X Annexin binding buffer were added and analyzed by flow cytometry within 1 h. The signal intensity was measured using a FACSARIA BD and analyzed using FASCDIVA BD.

4.4.3. Propidium iodide staining of DNA content and cell cycle analyses

Human Caco-2 cell line PD7 and TC7 clones were exposed for 72 h with 20 μM of the metallic compounds. Cells were fixed in 70% ice-cold ethanol and stored at 4 °C for 24 h. After centrifugation, cells were rehydrated in PBS (phosphated buffered saline) and stained in propidium iodide (PI, 50 μg/mL) solution containing RNase A (100 μg/mL). PI stained cells were analyzed for DNA content in a FACSARRAY BD equipped with an argon ion laser. The red fluorescence emitted by PI was collected by 620 nm longer pass filter, as a measure of the amount of DNA-bound PI and displayed on a linear scale. Cell cycle distribution was determined on a linear scale. The percentage of cells in cycle phases was determined using MODIFIT 3.0 verity software.

4.4.4. Solution chemistry

The stability of [Au(Spyrim)(PTA–CH_2Ph)]Br (**4a**) in buffer solution was analyzed by absorption UV–visible spectroscopy. The complex was dissolved in DMSO (10 mM) and diluted in the reference PBS buffer, at pH 7.4, to a final concentration of 1×10^{-4} M, and the sample was analyzed spectrophometrically over 24 h at 37 °C.

Acknowledgments

Authors thank to Centro de Investigación Biomédica de Aragón (CIBA), España for the technical assistance: http://www.ics.aragon.es and to Torrecid S.A. for a generous donation of H[$AuCl_4$].

Appendix A. Supplementary data

Supplementary data related to this article can be found at http://dx.doi.org/10.1016/j.ejmech.2014.04.001.

References

[1] S.P. Fricker, Gold Bulletin 29 (1996) 53–60.
[2] C. Orvig, M.J. Abrams, Chemical Reviews 99 (1999) 2201–2203.
[3] E.R.T. Tiekink, Gold Bulletin 36 (2003) 117–124.
[4] J.E. Pope, P. Hong, B.E. Koehler, Journal of Rheumatology 29 (2002) 255–260.
[5] A.J. Lehman, J.M. Esdaile, A.V. Klinkhoff, E. Grant, A. Fitzgerald, J. Canvin, Arthritis & Rheumatism 52 (2005) 1360–1370.
[6] B.M. Sutton, E. McGusty, D.T. Waltz, M.J. Di Martino, Journal of Medicinal Chemistry 15 (1972) 1095–1098.
[7] B.M. Sutton, Gold Bulletin 19 (1986) 15–16.
[8] T. Okada, B.K. Patterson, S.Q. Ye, M.E. Gurney, Virology 192 (1993) 631–642.
[9] K. Yamaguchi, H. Ushijima, M. Hisano, Y. Inoue, T. Shimamura, T. Hirano, W.E.G. Muller, Microbiology and Immunology 45 (2001) 549–555.
[10] R.E. Thomas, R.A. Papandrea, Medical Journal of Australia 158 (1993) 720.
[11] M. Navarro, H. Perez, R.A. Sanchez-Delgado, Journal of Medicinal Chemistry 40 (1997) 1937–1939.
[12] M. Navarro, E.J. Cisneros-Fajardo, T. Lehmann, R.A. Sanchez-Delgado, R. Atencio, P. Silva, R. Lira, J.A. Urbina, Inorganic Chemistry 40 (2001) 6879–6884.
[13] M.J. McKeage, L. Maharaj, S.J. Berners-Price, Coordination Chemistry Reviews 232 (2002) 127–135.
[14] S. Nobili, E. Mini, I. Landini, C. Gabbiani, A. Casini, L. Messori, Medicinal Research Reviews 30 (2010) 550–580.
[15] I. Ott, Coordination Chemistry Reviews 253 (2009) 1670–1681.
[16] T.M. Simon, D.H. Kunishima, G.J. Vibert, A. Lorber, Cancer Research 41 (1981) 94–97.
[17] T.M. Simon, D.H. Kunishima, G.J. Vibert, A. Lorber, Cancer 44 (1979) 1965–1975.
[18] C.K. Mirabelli, R.K. Johnson, C.-M. Sung, L.F. Faucette, K. Murihead, S.T. Crooke, Cancer Research 45 (1985) 32–39.
[19] C.F. Shaw, Chemical Reviews 99 (1999) 2589–2600.
[20] S.J. Berners-Price, A. Filipovska, Metallomics 3 (2011) 863–873.
[21] C.-M. Che, R.W.-Y. Sun, C.B. Ko, N. Zhu, H. Sun, Chemical Communications (2003) 1718.
[22] E.R.T. Tiekink, Inflammopharmacology 16 (2008) 138–142.
[23] W.F. Kean, I.R.L. Kean, Inflammopharmacology 16 (2008) 112–125.
[24] V. Milacic, D. Fregona, Q.P. Dou, Histology and Histopathology 23 (2008) 101–108.
[25] R.W.-Y. Sun, C.-M. Che, Coordination Chemistry Reviews 253 (2009) 1682–1691.
[26] I. Kostova, Anti-Cancer Agents in Medicinal Chemistry 6 (2006) 19–32.
[27] P.J. Barnard, S.J. Berners-Price, Coordination Chemistry Reviews 251 (2007) 1889–1902.
[28] A. Casini, Journal of Inorganic Biochemistry 109 (2012) 97–106.
[29] G.D. Hoke, G.F. Rush, G.E. Bossard, J.V. McArdle, B.D. Jensen, C.K. Mirabelli, Journal of Biological Chemistry 263 (1988) 11203–11210.
[30] G.D. Hoke, R.A. Macia, P.C. Meunier, P.J. Bugelski, C.K. Mirabelli, G.F. Rush, W.D. Matthews, Toxicology and Applied Pharmacology 100 (1989) 293–306.
[31] P.F. Smith, G.D. Hoke, D.W. Alberts, P.J. Bugelski, S. Lupo, C.K. Mirabelli, G.F. Rush, Journal of Pharmacology and Experimental Therapeutics 249 (1989) 944–950.
[32] J.J. Liu, P. Galettis, A. Farr, L. Maharaj, H. Samarasinha, A.C. McGechan, B.C. Baguley, R.J. Bowen, S.J. Berners-Price, M.J. McKeage, Journal of Inorganic Biochemistry 102 (2008) 303–310.
[33] A.S. Humphreys, A. Filipovska, S.J. Berners-Price, G.A. Koutsantonis, B.W. Skelton, A.H. White, Dalton Transactions (2007) 4943–4950.
[34] S.J. Berners-Price, R.J. Bowen, P. Galettis, P.C. Healy, M.J. McKeage, Coordination Chemistry Reviews 185-6 (1999) 823–836.
[35] M.J. McKeage, S. Berners-Price, P. Galettis, R.J. Bowen, W. Brouwer, L. Ding, L. Zhuang, B.C. Baguley, Cancer Chemotherapy and Pharmacology 46 (2000) 343–350.
[36] D. Screnci, M.J. McKeage, P. Galettis, T.W. Hambley, B.D. Palmer, B.C. Baguley, British Journal of Cancer 82 (2000) 966–972.
[37] E. Vergara, E. Cerrada, C. Clavel, A. Casini, M. Laguna, Dalton Transactions 40 (2011) 10927–10935.

[38] S. Miranda, E. Vergara, F. Mohr, D. de Vos, E. Cerrada, A. Mendia, M. Laguna, Inorganic Chemistry 47 (2008) 5641–5648.
[39] E. Vergara, A. Casini, F. Sorrentino, O. Zava, E. Cerrada, M.P. Rigobello, A. Bindoli, M. Laguna, P.J. Dyson, ChemMedChem 5 (2010) 96–102.
[40] E. Vergara, S. Miranda, F. Mohr, E. Cerrada, E.R.T. Tiekink, P. Romero, A. Mendia, M. Laguna, European Journal of Inorganic Chemistry (2007) 2926–2933.
[41] E. Vergara, E. Cerrada, A. Casini, O. Zava, M. Laguna, P.J. Dyson, Organometallics 29 (2010) 2596–2603.
[42] E. Garcia-Moreno, S. Gascon, M.J. Rodriguez-Yoldi, E. Cerrada, M. Laguna, Organometallics 32 (2013) 3710–3720.
[43] E. García-Moreno, E. Cerrada, M.J. Bolsa, A. Luquin, M. Laguna, European Journal of Inorganic Chemistry (2013) 2020–2030.
[44] S. Schäfer, W. Frey, A.S.K. Hashmi, V. Cmrecki, A. Luquin, M. Laguna, Polyhedron 29 (2010) 1925–1932.
[45] A. Mena-Cruz, P. Lorenzo-Luis, A. Romerosa, M. Saoud, M. Serrano-Ruiz, Inorganic Chemistry 46 (2007) 6120–6128.
[46] A. Mena-Cruz, P. Lorenzo-Luis, A. Romerosa, M. Serrano-Ruiz, Inorganic Chemistry 47 (2008) 2246–2248.
[47] E. Cerrada, E.J. Fernandez, M.C. Gimeno, A. Laguna, M. Laguna, R. Terroba, M.D. Villacampa, Journal of Organometallic Chemistry 492 (1995) 105–110.
[48] D.W. Allen, R. Berridge, N. Bricklebank, E. Cerrada, M.E. Light, M.B. Hursthouse, M. Laguna, A. Moreno, P.J. Skabara, Journal of the Chemical Society Dalton Transactions (2002) 2654–2659.
[49] M. Cera, E. Cerrada, M. Laguna, J.A. Mata, H. Teruel, Organometallics 21 (2002) 121–126.
[50] E. Cerrada, A. Moreno, M. Laguna, Dalton Transactions (2009) 6825–6835.
[51] M.N. Xanthopoulou, S.K. Hadjikakou, N. Hadjiliadis, M. Kubicki, S. Skoulika, T. Bakas, M. Baril, I.S. Butler, Inorganic Chemistry 46 (2007) 1187–1195.
[52] C.K. Mirabelli, C. Sung, M.H. Whitman, D.T. Hill, S. Mong, S.T. Crooke, Biochemical Pharmacology 35 (1986) 1427.
[53] A. de Almeida, B.L. Oliveira, J.D.G. Correia, G. Soveral, A. Casini, Coordination Chemistry Reviews 257 (2009) 2689–2704.
[54] A. Casini, Journal of Inorganic Biochemistry 109 (2013) 97–106.
[55] K.P. Bhabak, B.J. Bhuyan, G. Mugesh, Dalton Transactions 40 (2011) 2099–2111.
[56] A. Bindoli, M.P. Rigobello, G. Scutarib, C. Gabbiani, A. Casini, L. Messori, Coordination Chemistry Reviews 253 (2009) 1692–1707.
[57] L. Oehninger, R. Rubbiani, I. Ott, Dalton Transactions 42 (2013) 3269–3284.
[58] A. Citta, E. Schuh, F. Mohr, A. Folda, M.L. Massimino, A. Bindoli, A. Casini, M.P. Rigobello, Metallomics 5 (2013) 1006–1015.
[59] E. Schuh, C. Pfluger, A. Citta, A. Folda, M.P. Rigobello, A. Bindoli, A. Casini, F. Mohr, Journal of Medicinal Chemistry 55 (2012) 5518–5528.
[60] I. Romero-Canelon, P.J. Sadler, Inorganic Chemistry 52 (2013) 12276–12291.
[61] E. Martin, C. Spendley, A.J. Mountford, S.J. Coles, P.N. Horton, D.L. Hughes, M.B. Hursthouse, S.J. Lancaster, Organometallics 27 (2008) 1436–1446.
[62] C. Wetzel, P.C. Kunz, M.U. Kassak, A. Hamacher, P. Böhler, W. Watjen, I. Ott, R. Rubbiani, B. Spingler, Dalton Transactions 40 (2011) 9212–9220.
[63] J. Carmichael, W.G. Degraff, A.F. Gazdar, J.D. Minna, J.B. Mitchell, Cancer Research 47 (1987) 936–942.